



Photocatalytic Degradation of Crystal Violet Using CuFe_2O_4 in a Heterogeneous Photo-Fenton System with Ascorbic Acid

Apri Rahmanisa¹, Indang Dewata^{2*}, Mawardi³, Romy Dwipa Yamesa Away⁴

Chemistry Department, Faculty of Science and Education, Universitas Negeri Padang, Jl. Prof. Dr.

Hamka Air Tawar Barat, Padang, Indonesia

*Corresponding Author e-mail: indangdewata@fmipa.unp.ac.id

Article History

Received: 08-04-2026

Revised: 18-04-2026

Published: 30-04-2026

Keywords: Degradation; Crystal Violet; Photo-Fenton; CuFe_2O_4 , Ascorbic Acid.

Abstract

Crystal violet is a persistent dye that is difficult to remove using conventional treatment methods. This study investigates the degradation of crystal violet using a CuFe_2O_4 -based heterogeneous photo-Fenton system in the presence of ascorbic acid. The novelty of this work lies in the combined use of CuFe_2O_4 and ascorbic acid to enhance redox cycling and improve degradation performance under photo-Fenton conditions. The CuFe_2O_4 catalyst was synthesized via a sol-gel method and characterized using Fourier transform infrared (FTIR) spectroscopy and X-ray diffraction (XRD), confirming the formation of a spinel structure with an average crystallite size of 38.4 nm. The degradation process was evaluated by varying pH (1–9) and hydrogen peroxide (H_2O_2) concentration (10–50 mmol/L). The optimum pH was found to be 3, achieving a degradation efficiency of 94.38%, while the optimum H_2O_2 concentration was 30 mmol/L with a degradation efficiency of 93.56%. The improved degradation performance is attributed to enhanced hydroxyl radical ($\bullet\text{OH}$) generation facilitated by the interaction between CuFe_2O_4 and ascorbic acid. These results suggest that CuFe_2O_4 with ascorbic acid can improve crystal violet degradation under the tested photo-Fenton conditions.

How to Cite: Rahmanisa, A., Dewata, I., Mawardi, & Away, R. D. Y. (2026). Photocatalytic Degradation of Crystal Violet Using CuFe_2O_4 in a Heterogeneous Photo-Fenton System with Ascorbic Acid. *Hydrogen: Jurnal Kependidikan Kimia*, 14(2), 367-373. <https://doi.org/10.33394/hjkk.v14i2.20190>

 <https://doi.org/10.33394/hjkk.v14i2.20190>

This is an open-access article under the [CC-BY-SA License](https://creativecommons.org/licenses/by-sa/4.0/).



INTRODUCTION

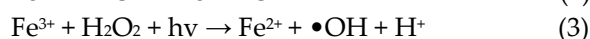
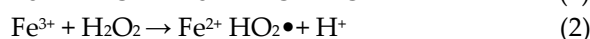
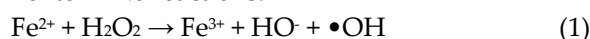
The discharge of dye-containing wastewater from industrial activities, particularly in textile and printing sectors, has become a significant environmental concern due to its persistence and resistance to conventional treatment methods (X. Zhang et al., 2020). Among various dyes, crystal violet is widely used but is known for its high toxicity, stability, and potential carcinogenic effects, making it hazardous to aquatic ecosystems and human health (Katheresan et al., 2018).

Advanced oxidation processes (AOPs) have been extensively studied for the removal of such persistent organic pollutants. Among them, the photo-Fenton process is considered a promising approach due to its ability to generate highly reactive hydroxyl radicals ($\bullet\text{OH}$) through the $\text{Fe}^{2+}/\text{Fe}^{3+}$ redox cycle in the presence of hydrogen peroxide (H_2O_2) under light irradiation (Pignatello et al., 2006; Deng & Zhao, 2015). These

radicals are capable of degrading complex organic molecules into simpler and less harmful compounds.

To improve the limitations of the conventional homogeneous Fenton system, such as sludge formation and difficulty in catalyst recovery, heterogeneous catalysts have been developed (Cao et al., 2019). Spinel ferrites, particularly CuFe_2O_4 , have attracted attention due to their structural stability, magnetic properties, and ability to facilitate redox reactions involving Fe and Cu species (Lasera et al., 202; Nidheesh, 2015).

The presence of dual active sites ($\text{Fe}^{3+}/\text{Fe}^{2+}$ and $\text{Cu}^{2+}/\text{Cu}^+$) enhances the catalytic performance in Fenton-like reactions.



In addition, the use of reducing agents such as ascorbic acid has been reported to accelerate the $\text{Fe}^{3+}/\text{Fe}^{2+}$ redox cycle, thereby increasing the generation of hydroxyl radicals and improving degradation efficiency (Markovskaya et al., 2015; Hou et al., 2016). However, studies combining CuFe_2O_4 with ascorbic acid in a heterogeneous photo-Fenton system for crystal violet degradation remain limited, particularly in terms of optimizing operational parameters.

Therefore, this study aims to synthesize CuFe_2O_4 and evaluate the effects of pH and H_2O_2 concentration on crystal violet degradation in a heterogeneous photo-Fenton system assisted by ascorbic acid. This work is expected to provide further insight into the role of catalyst–reductant interaction in enhancing degradation performance.

METHOD

Material and Instruments

The materials used were crystal violet ($\text{C}_{25}\text{H}_{30}\text{ClN}_3$), copper nitrate trihydrate ($\text{Cu}(\text{NO}_3)_2 \cdot \text{H}_2\text{O}$), iron(III) nitrate nonahydrate ($\text{Fe}(\text{NO}_3)_3 \cdot 9\text{H}_2\text{O}$), citric acid monohydrate ($\text{C}_6\text{H}_8\text{O}_7 \cdot \text{H}_2\text{O}$), ammonia (NH_3), Sulfuric acid (H_2SO_4 , 0.1 M) and sodium hydroxide (NaOH , 0.1 M), Hydrogen peroxide (H_2O_2 , 30%), ascorbic acid ($\text{C}_6\text{H}_8\text{O}_6$), Distilled water, methanol, alcohol, and filter paper. The instruments used in this study included a beaker, volumetric flask, volumetric pipette, dropper pipette, funnel, thermometer, glass stirring rod, spatula, evaporating dish, graduated cylinder, 5 W UV lamp, glass batch reactor (800 mL capacity), pH meter, oven, desiccator, furnace, spin bar, centrifuge, test tubes, magnetic stirrer, UV–Vis spectrophotometer, Fourier transform infrared (FTIR) spectrometer, and X-ray diffraction (XRD) instrument.

Catalyst Synthesis

CuFe_2O_4 nanoparticles were synthesized using the sol–gel method. First, copper nitrate trihydrate ($\text{Cu}(\text{NO}_3)_2 \cdot \text{H}_2\text{O}$) and iron(III) nitrate nonahydrate ($\text{Fe}(\text{NO}_3)_3 \cdot 9\text{H}_2\text{O}$) were dissolved in 50 mL of distilled water with concentrations of 0.1 mol/L and 0.2 mol/L, respectively. Then, 0.3 mol of citric acid monohydrate was added to the solution and stirred thoroughly for 5 minutes at room temperature. Next, Ammonia (NH_3) was then added to adjust the pH to 7, and the mixture was continuously stirred at 70°C for 7 hours, resulting in the gradual formation of a green gel. The obtained gel was dried at 130°C for 7 hours

and then calcined in a furnace at 600°C for 3 hours. The resulting product was washed three times with distilled water and three times with alcohol. Finally, the washed product was dried to obtain the desired CuFe_2O_4 nanoparticles.

Determination of Optimum pH

A crystal violet solution with a concentration of 10 mg/L was prepared and transferred into a 250 mL beaker, which served as the reactor. The pH of the solution was adjusted using 0.5 M H_2SO_4 and 0.5 M NaOH to obtain the desired pH values of 1, 3, 5, 7, and 9. After pH adjustment, the maximum absorption wavelength (λ_{max}) for each pH condition was determined using a UV–Vis spectrophotometer, and the initial absorbance (A_0) was recorded as a reference before the degradation process. Subsequently, 0.5 g of CuFe_2O_4 catalyst was added to the solution and stirred until homogeneous. The mixture was stirred in the dark for 30 minutes at 400 rpm to allow adsorption of crystal violet onto the catalyst surface. Afterward, hydrogen peroxide (H_2O_2) was added at a concentration of 30 mmol, followed by the addition of 1 mmol of ascorbic acid. The reaction was initiated by irradiation with a 5 W UV lamp to activate the photo-Fenton process, and the degradation was allowed to proceed for 60 minutes.

After the reaction, 9 mL of the sample was collected and mixed with 1 mL of methanol to effectively quench the photo-Fenton reaction. The mixture was then centrifuged for 5 minutes to separate the catalyst from the solution. The supernatant was analyzed using a UV–Vis spectrophotometer at the corresponding λ_{max} for each pH condition. The optimum pH was determined based on the highest degradation efficiency, and this value was used as the optimal condition for subsequent experiments.

Determination of Optimum H_2O_2 Concentration

A crystal violet solution with a concentration of 10 mg/L was transferred into a 250 mL beaker, which served as the reactor. The pH of the solution was adjusted to the optimum value obtained from the previous experiment using H_2SO_4 and NaOH solutions. The initial absorbance (A_0) was then measured using a UV–Vis spectrophotometer at the predetermined maximum wavelength (λ_{max}) as a reference before the degradation process. Subsequently, 0.5 g of CuFe_2O_4 catalyst was added to the solution and stirred using a magnetic stirrer at 400 rpm for

30 minutes in the dark to ensure adsorption equilibrium. After that, hydrogen peroxide (H_2O_2) was added with varying concentrations of 10, 20, 30, 40, and 50 mmol/L, along with 1 mmol/L of ascorbic acid. The reaction was initiated by irradiation with a 5 W UV lamp to activate the photo-Fenton process, and the degradation was allowed to proceed for 60 minutes.

After the reaction, 9 mL of the sample was collected and mixed with 1 mL of methanol to effectively quench the reaction. The mixture was then centrifuged for 5 minutes to separate the catalyst from the solution. The supernatant was analyzed using a UV-Vis spectrophotometer at the corresponding λ_{max} . The optimum H_2O_2 concentration was determined based on the highest degradation efficiency, and this condition was used for subsequent experiments.

Data Analysis

The data obtained from the measurements were in the form of absorbance values and were analyzed using the degradation efficiency equation.

$$D = \frac{A_0 - A_t}{A_0} \times 100\%$$

where D is the degradation efficiency (%), A_0 is the initial absorbance of crystal violet, and A_t is the absorbance at time t after the degradation process.

RESULTS AND DISCUSSION

FTIR Characterization

Fourier transform infrared (FTIR) analysis was conducted to identify the functional groups present in the synthesized CuFe_2O_4 . The formation of the material was indicated by the appearance of characteristic absorption bands associated with metal-oxygen bonds, which are active in the infrared region (Aslam et al., 2023). This method is widely used to confirm the formation of spinel ferrite structures due to its sensitivity toward metal-oxygen vibrations in the low wavenumber region ($400\text{--}600\text{ cm}^{-1}$) (Madhu & Rajendra prasad, 2025). The FTIR spectrum was recorded in the range of $4000\text{--}400\text{ cm}^{-1}$.

As shown in Figure 1, two prominent absorption bands were observed at approximately 536 cm^{-1} and 438 cm^{-1} , corresponding to Fe-O and Cu-O vibrations, respectively. These absorption bands are consistent with the intrinsic vibrational modes of spinel ferrites, where metal ions occupy tetrahedral and octahedral sites within the crystal

lattice (Surendra et al., 2018). The observed bands fall within the typical metal-oxygen vibration region ($400\text{--}600\text{ cm}^{-1}$), confirming the formation of the CuFe_2O_4 spinel structure (Peymanfar et al., 2018).

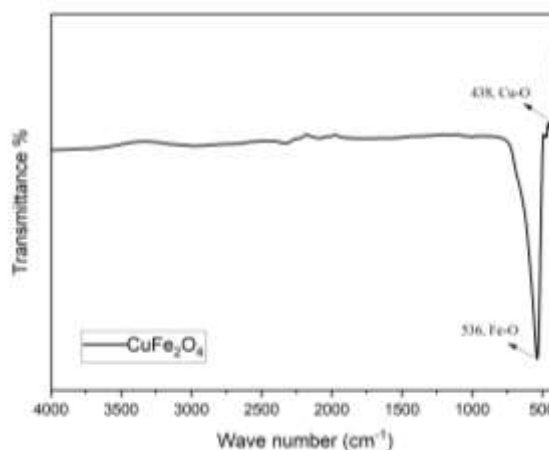


Figure 1. FTIR Spectra of CuFe_2O_4

When compared with previous studies, slight variations in the FTIR band positions are commonly reported due to differences in synthesis method, particle size, and calcination temperature. For instance, Jabbar et al., (2020) reported Fe-O and Cu-O stretching vibrations in CuFe_2O_4 prepared via sol-gel method at approximately 545 cm^{-1} and 460 cm^{-1} . Similarly, hydrothermally synthesized CuFe_2O_4 showed sharper and more intense absorption peaks, indicating higher crystallinity and improved cation distribution within the spinel structure (E. Zhang et al., 2019). The slight shift of absorption bands in the present study may be attributed to differences in crystallite size and degree of structural ordering. Nevertheless, the obtained FTIR results strongly confirm the successful formation of CuFe_2O_4 with a well-defined spinel ferrite structure.

XRD Characterization

The X-ray diffraction (XRD) pattern of the synthesized CuFe_2O_4 reveals several distinct diffraction peaks at 2θ values of approximately 18.40° , 29.94° , 30.81° , 34.55° , 36.12° , 41.50° , 44.17° , 54.20° , and 57.19° . These reflections can be indexed to the (111), (220), (311), (422), (511), and (440) crystal planes, which are characteristic of a cubic spinel ferrite structure. Among all peaks, the (311) reflection exhibits the highest intensity, indicating that this plane is the most preferred orientation and confirming the successful formation of the CuFe_2O_4 spinel phase (Güner et al., 2014).

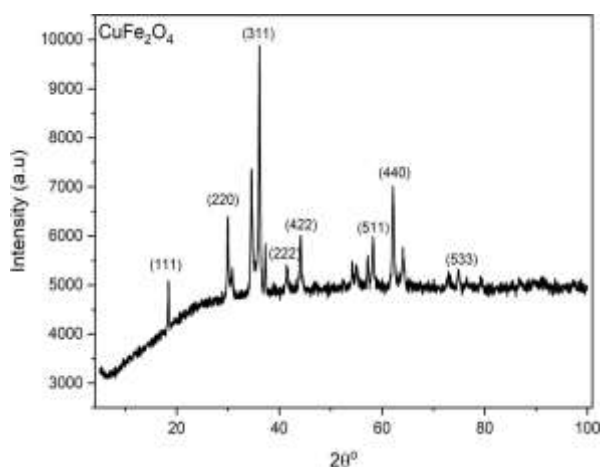


Figure 2. Diffractogram of CuFe_2O_4

The absence of additional diffraction peaks corresponding to secondary phases such as CuO or Fe_2O_3 suggests that the synthesized material is highly phase-pure. This indicates that the synthesis route effectively promoted complete reaction between copper and iron precursors, preventing the formation of detectable impurities. Similar findings were reported by (Базаргов et al., 2012) who emphasized that optimized synthesis conditions lead to the formation of single-phase CuFe_2O_4 with sharp and well-defined spinel peaks without impurity signals.

The observed diffraction pattern is in good agreement with previous literature. Feng & Ying, (2023) reported that CuFe_2O_4 typically exhibits strong diffraction peaks in the range of 30° – 60° , particularly associated with the (220), (311), and (440) planes, which closely match the results obtained in this study. Likewise, E. Zhang et al., (2019) demonstrated that hydrothermally synthesized CuFe_2O_4 shows dominant (311) and (440) reflections, which are strongly associated with high crystallinity and improved catalytic activity. High crystallinity is known to enhance electron transfer efficiency, which is crucial for catalytic and photocatalytic applications such as Fenton-like reactions and dye degradation processes.

Furthermore, Ferreira et al., (2022) reported that synthesis parameters such as calcination temperature significantly influence peak intensity and crystallinity of CuFe_2O_4 . Their study confirmed that stronger and sharper (311) peaks are indicative of improved crystal ordering, which is consistent with the results observed in this work. The crystallite size calculated using the Debye–Scherrer equation was approximately 38.4 nm, indicating that the synthesized CuFe_2O_4 falls within the nanocrystalline range.

Effect of pH on Crystal Violet Degradation

The degradation of crystal violet using the photo-Fenton method was first evaluated by determining the optimal pH. The experiments were initially conducted under dark conditions and subsequently irradiated with a 5 W UV lamp. The degradation performance at different pH values (1, 3, 5, 7, and 9) was monitored using a UV–Vis spectrophotometer at the corresponding maximum wavelength (λ_{max}) for each condition.

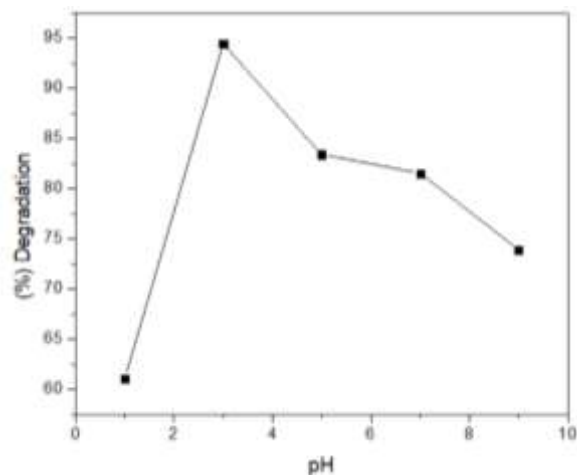


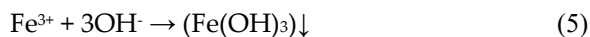
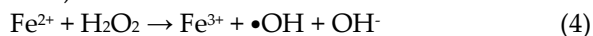
Figure 3. Degradation pH variation

As illustrated in Figure 3, the highest degradation efficiency was obtained at pH 3 (94.38%), suggesting that acidic conditions markedly improve the performance of the photo-Fenton process. When the pH increased, a decline in efficiency was observed, which can be attributed to the formation of iron hydroxide precipitates. This phenomenon reduces the concentration of dissolved iron species and subsequently suppresses hydroxyl radical ($\bullet\text{OH}$) formation (Fan et al., 2009).

The superior activity at pH 3 is associated with the enhanced $\text{Fe}^{2+}/\text{Fe}^{3+}$ redox cycling under acidic conditions, which promotes continuous decomposition of H_2O_2 and sustained generation of $\bullet\text{OH}$ radicals. Furthermore, the CuFe_2O_4 catalyst also participates through the $\text{Cu}^{2+}/\text{Cu}^+$ redox pair, contributing to additional radical production. Under these conditions, both iron and copper species remain soluble and catalytically active, resulting in more effective degradation of crystal violet (X. Zhang et al., 2020).

In contrast, at pH values above 5, the degradation performance decreased considerably due to the precipitation of $\text{Fe}(\text{OH})_3$, which limits the availability of active iron species and disrupts the $\text{Fe}^{2+}/\text{Fe}^{3+}$ catalytic cycle. In addition, the instability of H_2O_2 in alkaline media further

reduces the formation of $\bullet\text{OH}$ radicals, leading to lower overall oxidation efficiency (Wu et al., 2010).



CuFe_2O_4 acts as a heterogeneous catalyst containing two main active sites, namely Fe^{3+} and Cu^{2+} ions on its surface. Under acidic conditions, particularly at pH 3, these surface metal ions are more easily reduced. Fe^{3+} species are reduced to Fe^{2+} , while Cu^{2+} is reduced to Cu^+ . These reduced metal centers play a crucial role in activating hydrogen peroxide (H_2O_2) to generate highly reactive hydroxyl radicals ($\bullet\text{OH}$) through Fenton-like reactions (Fatmawati et al., 2025).

Effect of H_2O_2 Concentration on Crystal Violet Degradation

After determining the optimal pH (pH 3), the effect of hydrogen peroxide concentration was investigated by varying its concentration from 10 to 50 mmol/L. The degradation process was conducted under dark conditions followed by UV irradiation for 60 minutes, and the analysis was performed using UV-Vis spectrophotometry at the λ_{max} corresponding to pH 3.

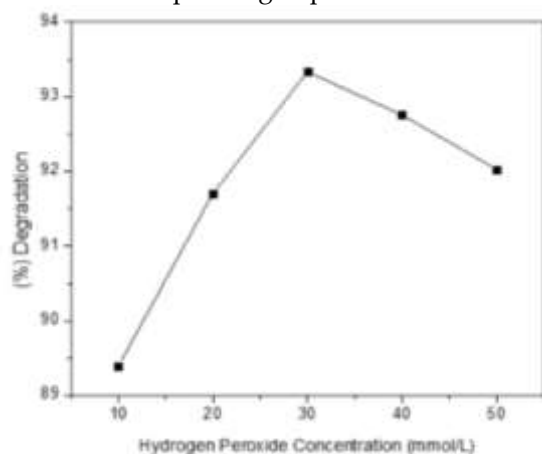


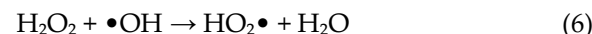
Figure 4. Degradation of H_2O_2 variation

Figure 4, the degradation efficiency increased with increasing H_2O_2 concentration up to an optimum value. The highest degradation efficiency was obtained at 30 mmol/L, reaching 93.33%. Increasing the H_2O_2 concentration from 10 to 30 mmol/L enhanced the degradation efficiency, indicating improved hydroxyl radical generation. However, further increase to 50 mmol/L resulted in a slight decrease in efficiency. This behavior can be explained by the dual role of H_2O_2 in the photo-Fenton system. At low concentrations, H_2O_2 promotes the formation

of $\bullet\text{OH}$ radicals, thereby enhancing degradation. In contrast, excessive H_2O_2 acts as a scavenger that reacts with $\bullet\text{OH}$ radicals, reducing their availability for oxidation reactions and decreasing overall efficiency (Xue et al., 2009). Therefore, an optimal concentration of H_2O_2 is required to balance radical generation and consumption.

The selected range of hydrogen peroxide (H_2O_2) concentrations (10–50 mmol/L) was based on the typical operating conditions of Fenton and photo-Fenton systems, in which H_2O_2 acts as the primary precursor for hydroxyl radical ($\bullet\text{OH}$) generation. At low concentrations, the amount of H_2O_2 is insufficient to produce an adequate number of reactive radicals, resulting in limited dye degradation efficiency (Dinesh et al., 2025). Conversely, excessive H_2O_2 may act as a radical scavenger, thereby reducing the overall oxidation performance. This concentration range is consistent with previous studies reporting that optimal H_2O_2 levels in Fenton-based systems generally fall within the tens of mmol/L range to achieve effective degradation performance (Li et al., 2013).

The decrease in degradation efficiency at higher H_2O_2 concentrations can be explained by radical scavenging reactions, as shown below.



The hydroperoxyl radical ($\text{HO}_2\bullet$) formed in this reaction possesses a lower oxidation potential compared to hydroxyl radicals ($\bullet\text{OH}$), resulting in reduced degradation efficiency toward organic pollutants. In addition, excess H_2O_2 may interfere with the $\text{Fe}^{2+}/\text{Fe}^{3+}$ catalytic cycle in the Fenton system, as Fe^{2+} is increasingly consumed without effectively generating additional $\bullet\text{OH}$ radicals. This disruption reduces catalyst regeneration efficiency and ultimately limits overall degradation performance (Xue et al., 2009).

CONCLUSION

This study demonstrated the successful degradation of crystal violet using a CuFe_2O_4 -based heterogeneous photo-Fenton system in the presence of ascorbic acid. The synthesized CuFe_2O_4 catalyst exhibited a spinel structure with an average crystallite size of approximately 38.4 nm, indicating its nanocrystalline nature.

The degradation efficiency was significantly influenced by operational parameters. The optimum pH was found to be 3, achieving a maximum degradation efficiency of 94.38%, while

the optimal hydrogen peroxide concentration was within the range of 10–50 mmol/L, with the highest degradation efficiency of 93.56% obtained at 30 mmol/L. The enhanced performance under acidic conditions and optimal oxidant concentration is attributed to the efficient generation of hydroxyl radicals ($\bullet\text{OH}$) in the photo-Fenton system.

Overall, the results indicate that the CuFe_2O_4 -based photo-Fenton process, assisted by ascorbic acid, is an effective approach for the degradation of dye pollutants and has strong potential for wastewater treatment applications.

RECOMMENDATION

Future research should prioritize a comprehensive evaluation of catalyst reusability to assess its long-term stability and practical feasibility. Furthermore, systematic investigations on the influence of catalyst dosage and ascorbic acid concentration are essential to optimize the reaction performance. Such studies are expected to provide deeper mechanistic insights and strengthen the potential application of this system in real-world wastewater treatment.

BIBLIOGRAPHY

- Aslam, A., Abid, M. Z., Rafiq, K., Rauf, A., & Hussain, E. (2023). Tunable sulphur doping on CuFe_2O_4 nanostructures for the selective elimination of organic dyes from water. *Scientific Reports*, 13(1), 1–13. <https://doi.org/10.1038/s41598-023-33185-0>
- Cao, Z., Zuo, C., & Wu, H. (2019). One step for synthesis of magnetic CuFe_2O_4 composites as photo-fenton catalyst for degradation organics. *Materials Chemistry and Physics*, 237 (April), 121842. <https://doi.org/10.1016/j.matchemphys.2019.121842>
- Deng, Y., & Zhao, R. (2015). Advanced Oxidation Processes (AOPs) in Wastewater Treatment. *Current Pollution Reports*, 1(3), 167–176. <https://doi.org/10.1007/s40726-015-0015-z>
- Dinesh, A., Radhakrishnan, K., Renuga, V., Patil, R. P., Rajadesingu, S., Suthakaran, S., Gunganathan, L., Ayyar, M., Santhamoorthy, M., Gnanasekaran, L., & Iqbal, M. (2025). Results in Chemistry Visible light photocatalytic degradation of tetracycline using copper ferrite nanoparticles synthesized via Glycine-Assisted combustion method. *Results in Chemistry*, 13 (October 2024), 102037. <https://doi.org/10.1016/j.rechem.2025.102037>
- Fan, H. J., Huang, S. T., Chung, W. H., Jan, J. L., Lin, W. Y., & Chen, C. C. (2009). Degradation pathways of crystal violet by Fenton and Fenton-like systems: Condition optimization and intermediate separation and identification. *Journal of Hazardous Materials*, 171(1–3), 1032–1044. <https://doi.org/10.1016/j.jhazmat.2009.06.117>
- Fatmawati, R., Dewata, I., Nasra, E., & Away, R. D. Y. (2025). The efficiency of the Heterogeneous Photo-Fenton Process for Methyl Orange Degradation: A Review. *Jurnal Pijar MIPA*, 20(2), 325–333. <https://doi.org/10.29303/jpm.v20i2.8606>
- Feng, J., & Ying, Z. (2023). Ascorbic acid enhanced CuFe_2O_4 -catalyzed heterogeneous photo-Fenton-like degradation of phenol. *Journal of Environmental Engineering*.
- Ferreira, L. S., Silva, T. R., Silva, V. D., Raimundo, R. A., Simões, T. A., Loureiro, F. J. A., Fagg, D. P., Morales, M. A., & Macedo, D. A. (2022). Spinel ferrite MFe_2O_4 (M = Ni, Co, or Cu) nanoparticles prepared by a proteic sol-gel route for oxygen evolution reaction. *Advanced Powder Technology*, 33(1), 103391. <https://doi.org/10.1016/j.apt.2021.12.010>
- Güner, S., Esir, S., Baykal, A., Demir, A., & Bakis, Y. (2014). Magneto-optical properties of $\text{Cu}_{1-x}\text{Zn}_x\text{Fe}_2\text{O}_4$ nanoparticles. *Superlattices and Microstructures*, 74, 184–197. <https://doi.org/10.1016/j.spmi.2014.06.021>
- Hou, X., Huang, X., Ai, Z., Zhao, J., & Zhang, L. (2016). Ascorbic acid/ $\text{Fe@Fe}_2\text{O}_3$: A highly efficient combined Fenton reagent to remove organic contaminants. *Journal of Hazardous Materials*, 310(i), 170–178. <https://doi.org/10.1016/j.jhazmat.2016.01.020>
- Jabbar, R., Sabeh, S., & Hameed, A. (2020). Synthesis and Characterization of CoFe_2O_4 Nanoparticles Prepared by Sol-Gel Method. *Engineering and Technology Journal*, 38(2B), 47–53. <https://doi.org/10.30684/etj.v38i2b.252>
- Katheresan, V., Kansedo, J., & Lau, S. Y. (2018). Efficiency of various recent wastewater dye removal methods: A review. *Journal of Environmental Chemical Engineering*, 6(4), 4676–4697. <https://doi.org/10.1016/j.jece.2018.06.060>
- Lasera, A. G., Aritonang, H., & Koleangan, H. (2020). Sintesis dan Karakterisasi Nanopartikel CuFe_2O_4 serta Aplikasinya sebagai Antibakteri. *Chemistry Progress*, 12(2). <https://doi.org/10.35799/cp.12.2.2019.27929>
- Li, Y., Kawashima, N., Li, J., Chandra, A. P., & Gerson, A. R. (2013). A review of the structure, and fundamental mechanisms and kinetics of the leaching of chalcopyrite. *Advances in Colloid and Interface Science*, 197–198, 1–32. <https://doi.org/10.1016/j.cis.2013.03.004>
- Madhu, H., & Rajendra prasad, S. (2025). Green synthesis and reflux method of CuFe_2O_4 and Clay/ CuFe_2O_4 nanocomposite for photocatalysis and antioxidant studies. *Chemistry of Inorganic Materials*, 6 (November 2024), 100099. <https://doi.org/10.1016/j.cinorg.2025.100099>
- Markovskaya, D. V., Cherepanova, S. V., Saraev, A. A., Gerasimov, E. Y., & Kozlova, E. A. (2015).

- Photocatalytic hydrogen evolution from aqueous solutions of $\text{Na}_2\text{S}/\text{Na}_2\text{SO}_3$ under visible light irradiation on $\text{CuS}/\text{Cd}_{0.3}\text{Zn}_{0.7}\text{S}$ and $\text{Ni}_2\text{Cd}_{0.3}\text{Zn}_{0.7}\text{S}_{1+z}$. *Chemical Engineering Journal*, 262, 146–155. <https://doi.org/10.1016/j.cej.2014.09.090>
- Nidheesh, P. V. (2015). Heterogeneous Fenton catalysts for the abatement of organic pollutants from aqueous solution: A review. *RSC Advances*, 5(51), 40552–40577. <https://doi.org/10.1039/c5ra02023a>
- Peymanfar, R., Azadi, F., & Yassi, Y. (2018). Preparation and Characterization of CuFe_2O_4 Nanoparticles by the Sol-Gel Method and Investigation of Its Microwave Absorption Properties at Ku-Band Frequency Using Silicone Rubber. 1155. <https://doi.org/10.3390/ecms2018-05218>
- Pignatello, J. J., Oliveros, E., & MacKay, A. (2006). Advanced oxidation processes for organic contaminant destruction based on the fenton reaction and related chemistry. *Critical Reviews in Environmental Science and Technology*, 36(1), 1–84. <https://doi.org/10.1080/10643380500326564>
- Surendra, B. S., Veerabhadrswamy, M., Anantharaju, K. S., Nagaswarupa, H. P., & Prashantha, S. C. (2018). Green and chemical-engineered CuFe_2O_4 : characterization, cyclic voltammetry, photocatalytic and photoluminescent investigation for multifunctional applications. *Journal of Nanostructure in Chemistry*, 8(1), 45–59. <https://doi.org/10.1007/s40097-018-0253-x>
- Wu, H., Fan, M. M., Li, C. F., Peng, M., Sheng, L. J., Pan, Q., & Song, G. W. (2010). Kinetic studies on the degradation of crystal violet by the Fenton oxidation process. *Water Science and Technology*, 62(1), 1–7. <https://doi.org/10.2166/wst.2010.170>
- Xue, X., Hanna, K., & Deng, N. (2009). Fenton-like oxidation of Rhodamine B in the presence of two types of iron (II, III) oxide. *Journal of Hazardous Materials*, 166(1), 407–414. <https://doi.org/10.1016/j.jhazmat.2008.11.089>
- Zhang, E., Wang, L., Zhang, B., Xie, Y., & Wang, G. (2019). Shape-controlled hydrothermal synthesis of CuFe_2O_4 nanocrystals for enhancing photocatalytic and photoelectrochemical performance. *Materials Chemistry and Physics*, 235. <https://doi.org/10.1016/j.matchemphys.2019.05.021>
- Zhang, X., Geng, Z., Jian, J., He, Y., Lv, Z., Liu, X., & Yuan, H. (2020). Potassium ferrite as heterogeneous photo-fenton catalyst for highly efficient dye degradation. *Catalysts*, 10(3). <https://doi.org/10.3390/catal10030293>
- Балагуров, А. М., Бобриков, И. А., Мащенко, М. С., Сангаа, Д., Симкин, В. Г., & Суфе, В. Ш. (2012). Р 14-2012-124 СТРУКТУРНЫЙ ФАЗОВЫЙ ПЕРЕХОД.